

Application of Force and Inertial Sensors to Monitor the Usage of Walker Assistive Devices

Vítor Viegas^{1,2,3}, J. M. Dias Pereira^{1,2}, Octavian Postolache^{1,4}, Pedro Silva Girão^{1,5}

¹*Instituto de Telecomunicações, Lisboa, Portugal*

²*ESTSetúbal/³CDP2T, Instituto Politécnico de Setúbal, Setúbal, Portugal*

⁴*ISCTE – Instituto Universitário de Lisboa, Lisboa, Portugal*

⁵*Instituto Superior Técnico, Universidade de Lisboa, Lisboa, Portugal*

Email: vitor.viegas@estsetubal.ips.pt

Abstract – Walker assistive devices should be used properly in order to provide maximum safety and comfort to the user. We define two risk indexes to monitor walker usage, one related with force unbalance, and the other related with motor incoordination. We present a measurement system capable of measuring these two indexes and prevent potential risk situations. Force unbalance is measured using load cells attached to the walker legs. Motor incoordination is estimated by synchronizing force measurements with kinematic data provided by an Inertial Measurement Unit (IMU). The measurement system is equipped with a Bluetooth link that enables local supervision on a computer or smartphone. Calibration and experimental results are included in the paper.

Keywords – walker assistive device; load cell; IMU; gait analysis; usage monitoring

I. INTRODUCTION

Assistive walking devices play an important role in maintaining and extending the autonomy and life quality of elderly people. They are also key elements in recovering the mobility of people affected by locomotion disabilities caused, for example, by amputation, cerebral palsy, injuries of spine or muscular dystrophies.

The mobility of elderly and disabled people is of real concern for modern societies. The proper usage of mobility aiding devices contributes to the sustainability of health and long-term care systems [1-2]. But the very same devices, when badly used, can be harmful and cause serious injuries [3-4]. The safety margin can be improved by educating users on how to use the equipment properly, and also by adding intelligence to the device in order to detect risk situations.

Several measurement solutions exist for this purpose [5-10], but many of them are too complex or too expensive or too impractical for day-to-day applications. We try to address these issues by designing a low-cost,

easy-adaptable instrumented walker that measures unbalance and detects, in real time, potential falling situations. We use load cells to measure the force applied on the legs, and an Inertial Measurement Unit (IMU) to sense motion. The acquired data is transferred through a Bluetooth link to a Personal Computer (PC) where it is processed.

The measurement methods and the technical solutions presented in this paper can inspire the instrumentation of other mobility aiding devices such as crutches, walking sticks, wheeled walkers and rollators. Care was taken to preserve the native functionality of the device and to minimize costs.

The paper is organized as follows: section II defines metrics to assess risk; section III explains how the risk is measured; section IV presents experimental results; and section V draws conclusions.

II. USAGE METRICS

In the next paragraphs we define two risk indexes that will be used to monitor walker usage and detect potential dangerous situations.

A. Force Balance

The first risk index (I_1) has to do with the (un)balance of forces applied on the walker legs.

Consider the coordinate system illustrated in Fig. 1 where the walker legs are numbered from 1 to 4 (as quadrants) and the y-axis points to the forward direction. According to this arrangement, the Center of Forces (COF) is given by:

$$COF_x = \frac{W_{12}(F_1 - F_2) + W_{43}(F_4 - F_3)}{2(F_1 + F_2 + F_3 + F_4)} \quad (1)$$

$$COF_y = \frac{L(F_1 - F_4) + L(F_2 - F_3)}{2(F_1 + F_2 + F_3 + F_4)} \quad (2)$$

where F_k represents the force applied on each leg, W_{12} and W_{43} represent the distances between the front and rear

legs respectively, which corresponds roughly to the mean walker width (W), and L represents the distance between front and rear legs, which corresponds to the walker length.

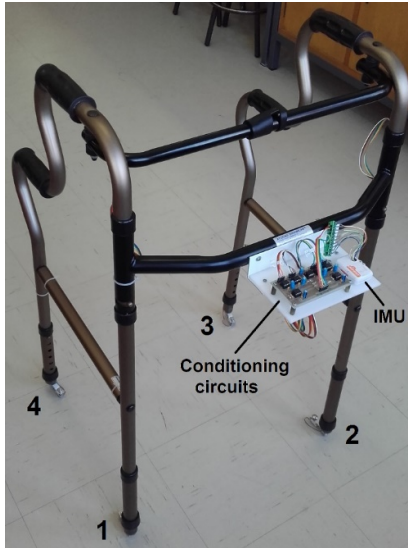
We define I_1 as the deviation of the COF in relation to the geometrical center of the walker polygon:

$$I_1(\%) = 100 \times \frac{\sqrt{(COF_x)^2 + (COF_y)^2}}{\sqrt{(W/2)^2 + (L/2)^2}} \times \alpha \quad (3)$$

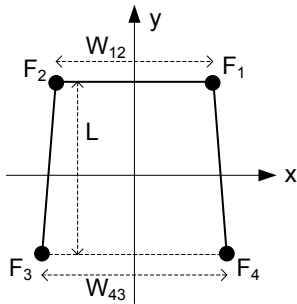
with α being given by:

$$\alpha = \frac{F_1 + F_2 + F_3 + F_4}{F_U} \quad (4)$$

where the numerator represents the total force applied on the walker legs and F_U represents the user weight. Alpha (α) is a weighting factor that takes values from 0 (when the walker is resting) to 1 (when the walker is charged with the weight of the user).

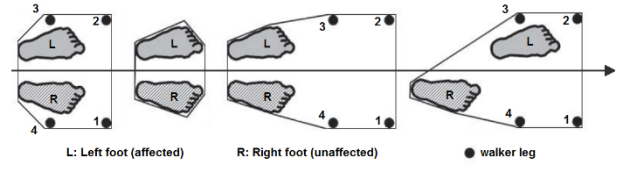


(a)

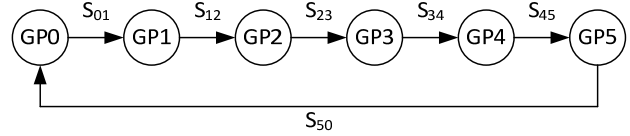


(b)

Fig. 1. Coordinate system chosen for the measurement system: a) Four-leg walker; b) Cartesian plane and dimensions.



(a)



(b)

Fig. 2. Walker step to gait phases: a) Animation (the polygon delimits the support area); b) State machine (GP0: the walker is resting on the floor; GP1: the walker is flying; GP2: the walker is on the floor waiting for the injured foot to move forward; GP3: the injured foot is moving forward; GP4: waiting for the healthy foot to move forward; GP5: the healthy foot is moving forward).

B. Motor Coordination

The second risk indicator (I_2) has to do with the (in) coordination between walker movements and user gait.

Consider the state machine illustrated in Fig. 2 where the states represent the Gait Phases (GP) and the continuous arrows represent normal transitions between states [11-12]. These transitions are validated by sensor measurements as follows:

- S_{01} is enabled if $F_1 + F_2 + F_3 + F_4 < \text{WEIGHT_TH}$ (threshold of minimum weight, value settable between 0 and the walker weight). This transition occurs when the total force measured by the load cells falls below the walker weight; in other words, when the walker is lifted in the air.
- S_{12} is enabled if $F_1 + F_2 + F_3 + F_4 > \text{WEIGHT_TH}$ and $d > \text{DISTANCE_TH}$ (threshold of minimum distance travelled forward, value settable between 4 cm and 40 cm). This transaction occurs when the walker touches down on the floor after traveling a distance greater than the minimum.
- S_{23} is enabled if $\text{COF}_x > \text{RIGHT_TH}$ or $\text{COF}_x < \text{LEFT_TH}$ depending on which foot is injured (left or right, respectively). This transaction occurs when the user moves forward the injured foot and applies maximum force on the opposite side. The injured foot is the first one to move forward. The type of disability must be defined in advance because it determines the threshold.
- S_{34} is enabled if $\text{COF}_x < \text{RIGHT_TH}$ or $\text{COF}_x > \text{LEFT_TH}$ depending on which foot is injured (left or right, respectively). This transaction occurs when the user alleviates the force previously applied

to the walker; in other words, when COF_x returns to zero.

- S₄₅ is enabled if COF_x < LEFT_TH or COF_x > RIGHT_TH depending on which foot is injured (left or right, respectively). This transaction occurs when the user moves forward the healthy foot and applies maximum force on the opposite side. The healthy foot is the last one to move forward.
- S₅₀ is enabled if COF_x > LEFT_TH or COF_x < RIGHT_TH depending on which foot is injured (left or right, respectively). This transaction occurs when the user alleviates the force previously applied to the walker; in other words, when COF_x returns to zero.

If the machine passes through all the states successfully then the step is marked as “good”. Otherwise, the step is marked as “bad” and the counter B is incremented. Then the incoordination index is computed as:

$$I_2(\%) = 100 \times \frac{B}{N} \quad (5)$$

where N is a moving window covering the last steps occurred (defaults to 10).

III. MEASUREMENT SYSTEM

The measurement system includes a set of load cells to sense force, an IMU to sense motion, a data acquisition board with Bluetooth link, and software to process data.

A. Force Sensors

Four load cells were used to measure the force applied on the walker legs. Each cell was attached to the extremity of a leg using a dedicated plastic adapter grown on a low-cost 3D printer (see Fig. 3). The cell contains 4 strain gauges fixed to a small body of aluminum (55.3x12.7x12.7mm) that supports 20 kgf. Other characteristics include: rate output = 1±0.15 mV/V, non-linearity = 0.05% FS, hysteresis = 0.05% FS, input impedance = 1130 Ω, output impedance = 1000 Ω, overload = 150% nominal capacity.

The use of bending beam load cells seems awkward when compared to inline/axial load cells. But the truth is that they are much cheaper making them the best choice for low-cost systems. The cell presented in Fig. 3 had a cost of 8 €.

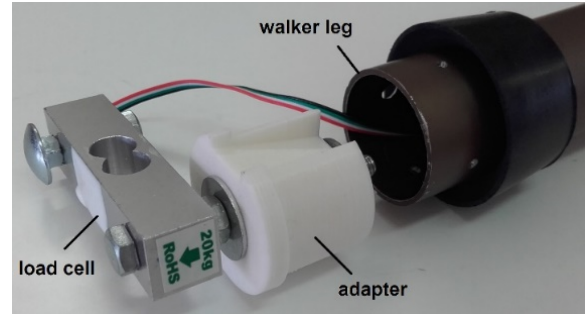


Fig. 3. Load cell attached to the walker leg.

Each load cell is supplied at 3 V and conditioned by an instrumentation amplifier with gain 100 (AD623), followed by a non-inverting amplifier with gain 8 (MCP6272). This gives an output swing from 0 to 2.4 V for forces between 0 and 20 kgf. The output is filtered by an RC low-pass filter with a cut-off frequency of 25 Hz.

B. Inertial Measurement Unit

Motion is sensed by an IMU, model Shimmer3 from Shimmer Sensing, attached to the walker body. The IMU has a pre-defined coordinate system that associates x, y and z axes to the length, width and height of its case, respectively. The IMU has nine degrees of freedom (9DoF) given by:

1. 3-axes accelerometer: model KXR5-2042 from Kionix, analog output, range = ±2 g, sensitivity = 600 mV/g, nonlinearity = 0.1% of full scale (FS).
2. 3-axes gyroscope: model MPU-9150 from Invensense, digital output, range = ±500 dps, sensitivity = 62.5 lsb/dps, nonlinearity = 0.2% FS.
3. 3-axes magnetometer: model LSM303DLHC from STMicroelectronics, digital output, range = ±4 Ga, sensitivity = 450 lsb/Ga for x and y axes and 400 lsb/Ga for the z axis, resolution = 2 mGa.

All sensors must be calibrated in advance to cancel offset errors and tune gain matrices. The calibration procedure [13] must be executed once and the calibration results must be saved into the non-volatile memory of the module.

The firmware of the IMU runs a gradient descent algorithm [14] that gives the orientation of the device in absolute ENU coordinates (local East-North-Up). This allows us to know the orientation of the walker and its horizontal acceleration.

C. Data Acquisition and Transmission

The Shimmer3 also acts as a wireless data acquisition board. It acquires data from all the sensors (four load cells plus the horizontal acceleration) at a rate of 51.2 S/s and sends it through a Bluetooth link. The data is then collected on the host side (computer or smartphone) and processed.

D. Data Processing

Data processing consists on the calculation of the risk indexes according to the following procedures:

1. Computation of COF_x and COF_y by solving equations (1) and (2).
2. Computation of the first risk index (I_1) by solving equations (3) and (4).
3. Detection of “bad” steps (B) by running the state machine represented in Fig. 2.
4. Computation of the second risk index (I_2) by solving equation (5).

All these tasks are done by the application “Spy Walker” that runs on the host side and is managed by the physiotherapist. The application, developed in Visual Studio 2012, makes use of ShimmerC# API [15] to interact with the Shimmer3 module. Its main window offers the following options (see Fig. 4):

- Login: Ask for information about the user, including identification, age and weight. The weight is needed to compute the α parameter in equation (4).
- Connect: Establish a Bluetooth link with the Shimmer3 module embedded in the walker.
- Calibrate Sensors: Open a sub-window intended to measure the walker weight (with the walker resting on the floor) and the biases associated to the COF and the walker weight (with the walker lifted in the air). The walker weight is used to compute the threshold WEIGHT_TH, and the biases are subtracted to cancel offsets.
- Stream Data: Open a sub-window where the physiotherapist can monitor, in real-time, the usage of the walker.
- Disconnect: Close the link with the shimmer3 module.

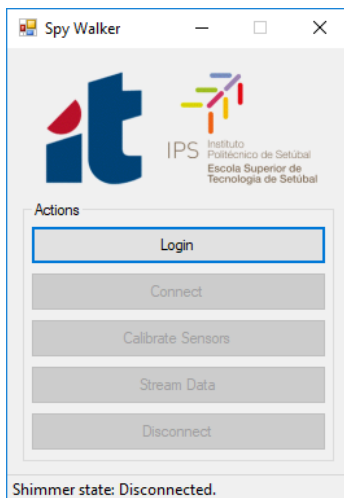
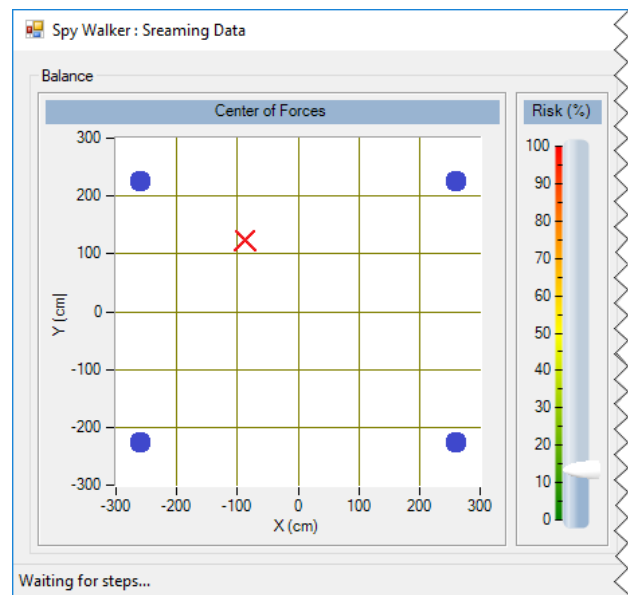


Fig. 4. Main window of the Spy Walker application.

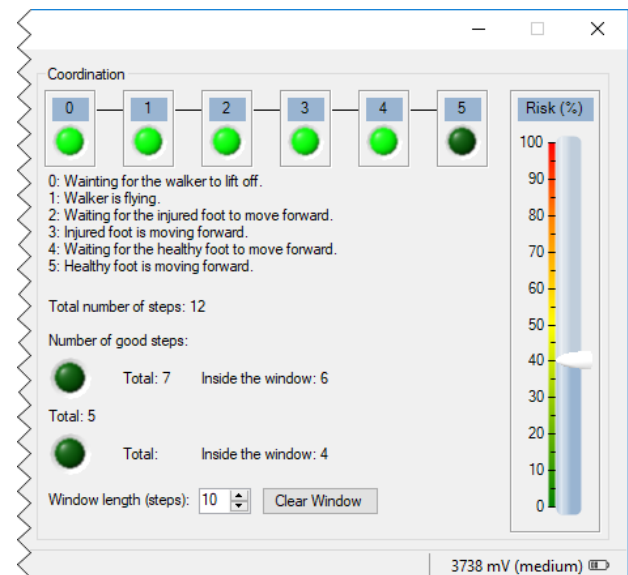
The Stream Data sub-window is where data

processing takes place. The graphical interface is divided in two main panels:

- Balance (see Fig. 5a): The COF is computed and the result is presented as a red cross moving over a XY graph. When the user loads his left side the cross moves toward negative values of X; when he loads his right side the cross moves toward positive values of X. The same applies for the front/back direction over the Y axis, much like a joystick. A vertical slider shows the instantaneous value of the I1 index.



(a)



(b)

Fig. 5. Stream Data sub-window: a) Panel for balance evaluation (the blue circles represent the walker legs); b) Panel for coordination evaluation.

Coordination (see Fig. 5b): The state machine is

executed and the current gait phase is identified. A set of six LEDs are turned on sequentially as the state machine moves forward the next phase. If the user passes through all the phases successfully, all the LEDs end up lighted and the step is marked as “good”. If the user violates any phase, the machine is reset to the first stage (GP0) and the step is marked as “bad”. The number of “good” and “bad” steps is registered. A vertical slider shows the instantaneous value of the I2 index.

IV. RESULTS AND DISCUSSIONS

The measurement system was tested by a user with impaired gait caused by an injury in the rightlower limb. The threshold value WEIGHT_TH was adjusted to half of the walker weight (known through calibration), and the threshold DISTANCE_TH was adjusted to 6 cm.

Fig. 6 shows the synchronized plots of d , COFx and I1 during a “good” step. Gait phase 0 was omitted because is a waiting state. During phase 1 the walker travels a distance $d \approx 20$ cm thus confirming the beginning of a new step. Phase 2 is a waiting state that ends when the user moves the injured foot (making COFx cross LEFT_TH). During phase 3 the user transfers part of his weight to the left in order to compensate the lack of support on the injured side. Then COFx returns to the origin and the machine moves to phase 4. This is another waiting state that ends when the user moves the healthy foot (making COFx cross RIGHT_TH). The load applied during phase 5 is lower than that applied on phase 3 because the healthy foot moves more easily than the injured foot.

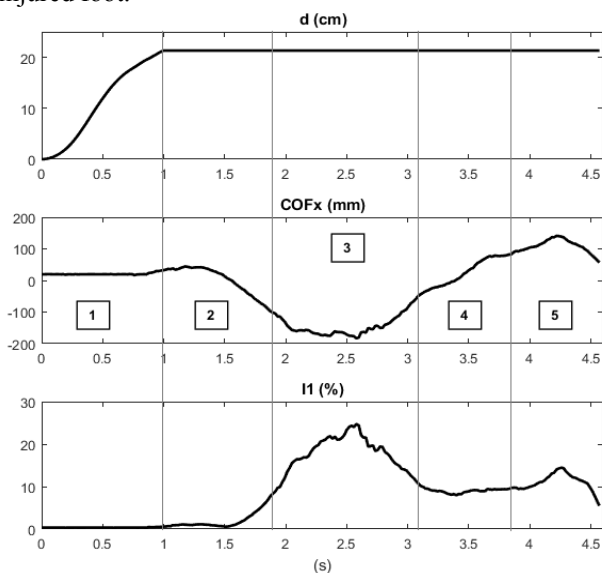


Fig. 6. Synchronized plots of d (top), COFx (middle) and I1 (bottom) during a “good” step. The square boxes numbered from 1 to 5 indicate gait phases. The threshold values are WEIGHT_TH = $0.5 \times$ WALKER_WEIGHT, DISTANCE_TH = 6 cm, LEFT_TH = -78 mm and RIGHT_TH = +78 mm.

Fig. 7 plots the number of “good” and “bad” steps inside a moving-window for a sequence of 20 steps. The window starts empty and covers the last 10 steps. It becomes full at the 10th step, with five “good” and five “bad” steps, which gives a value of 50% for I2. Thereafter the value of I2 tends to increase when a “bad” step is detected, or to decrease when a “good” step is detected instead.

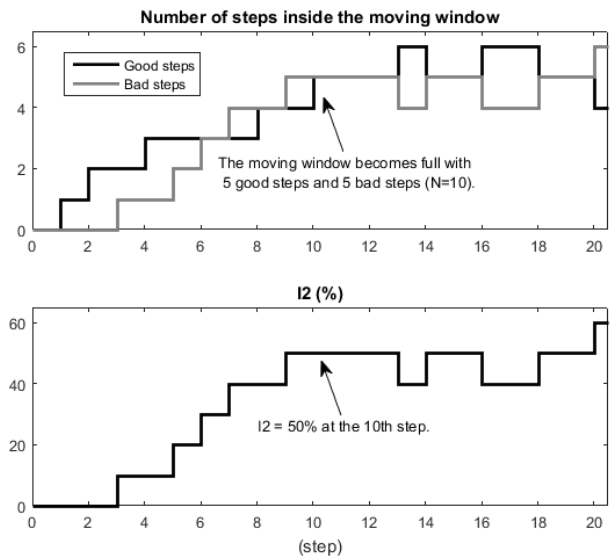


Fig. 7. Number of steps inside the moving window (top) and the corresponding value of I2 (bottom) for a sequence of 20 steps.

The step ends when both feet stay side-by-side making COFx return to the origin and restart the state machine. The state machine worked well with (very) few false “bads”. There were no false “goods” because the validation of a “good” step is very demanding. More work has to be done in order to improve the quality and robustness of the thresholds, including the study of adaptive tuning algorithms.

V. CONCLUSIONS

The experimental results confirm that is possible to monitor the usage of walker assistive devices combining force and inertial sensors. The sensed data is transmitted over a Bluetooth link and processed in real time, on the host side, in order to extract two risk indicators: I1 representing the (un)balance of forces applied on the walker legs, and I2 representing the (in)coordination between walker movements and user gait. Data processing and presentation is done by a Windows-based application managed by the physiotherapist. Experimental results demonstrate that risk indexes I₁ and I₂ are meaningful.

As future work we plan to introduce new functionalities to the measurement system. This includes automate of the login process (using smartcards or equivalent), give local feedback to the user (by

expressing I1 and I2 through colored LED strips or shaking the walker when the risk is too high), and extract more metrics from the IMU (including step height, ground orientation and velocities).

VI. ACKNOWLEDGMENT

The work was supported by Instituto de Telecomunicações and Fundação para a Ciência e Tecnologia, projects PTDC/DTPDES/1661/2012 and PTDC/DTP-DES/6776/2014.

REFERENCES

- [1] Sara M. Bradley, Cameron R. Hernandez, “Geriatric Assistive Devices”, *Am Fam Physician*, Issue 15, No. 84(4), pp. 405-411, August 2011.
- [2] S.R.Faruqi, T. Jaebon, “Ambulatory Assistive Devices in Orthopaedics: Uses and Modifications”, *J Am Acad Orthop Surg.*, Issue 18, No. 1, pp. 41–50, 2010.
- [3] H. Bateni, B. E. Maki, “Assistive Devices for Balance and Mobility: Benefits, Demands, and Adverse Consequences”, *Arch Phys Med Rehabil*, Issue 86, No. 1, pp. 134–145, 2005.
- [4] J.A. Stevens, K. Thomas, L. Teh, Greenspan et al, “Unintentional Fall Injuries Associated with Walkers and Canes in Older Adults Treated in U.S. Emergency Departments”, *J Am Geriatr Soc.*, Issue 57, No. 8, pp. 1464–1469, 2009.
- [5] D.D. Ely, G.L. Smidt, “Effect of Cane on Variables of Gait for Patients with Hip”, *Phys. Ther.*, No. 57, pp. 507-512, 1977.
- [6] Majd Alwan et al., “Basic Walker-Assisted Gait Characteristics Derived from Forces and Moments Exerted on the Walker’s Handles: Results on Normal Subjects”, *Medical Engineering and Physics*, No. 29, pp. 380-389, 2007.
- [7] Alvaro Muro-de-la-Herran, Begonya Garcia-Zapirain and Amaia Mendez-Zorrilla, “Gait Analysis Methods: An Overview of Wearable and Non-Wearable Systems, Highlighting Clinical Applications”, *Sensors Review*, 14, pp. 3362-3394, 2014.
- [8] Joel A. Delisa, Department of Veteran Affairs, “Rehabilitation Reserach and Development Service”, Chapter 2, pp. 11-32, 1981.
- [9] E.Sardini, M. Serpelloni, M. Lancini, “Wireless Instrumented Crutches for Force and Movement Measurements for Gait Monitoring”, *IEEE Transactions on Instrumentation and Measurement*, Vol. 64, No. 12, pp. 3369-3379, Dec. 2015.
- [10] J. M. Dias Pereira, Vítor Viegas, Octavian Postolache, Pedro Silva Girão, “Combining Distance and Force Measurements to Monitor the Usage of Walker Assistive Devices”, *IEEE International Instrumentation and Measurement Technology Conference (I2MTC)*, Torino, Italy, May 2017.
- [11] David A. Winter, “Biomechanics of Normal and Pathological Gait: Implications for Understanding Human Locomotor Control”, *Journal of Motor Behaviour*, Vol. 21, No. 4, pp. 337-355, December 1989.
- [12] Marder E, Calabrese RL, “Principles of Rhythmic Motor Pattern Generation”, *Physiological Reviews*, Vol. 76, Issue 3, 1996 Jul, 76(3):687–717.
- [13] “9DoF Calibration Application User Manual Rev. 2.5a”, Shimmer, 2014.
- [14] Sebastian O.H. Madgwick, Andrew J.L. Harrison, Ravi Vaidyanathan, “Estimation of IMU and MARG Orientation Using a Gradient Descent Algorithm”, 2011 IEEE International Conference on Rehabilitation Robotics, Zurich, Switzerland, June 29 - July 1.
- [15] “Shimmer C# API”, <http://www.shimmersensing.com/products/shimmercapture> (accessed the 5th of June 2017)